The Astrophysical Journal, 987:5 (10pp), 2025 July 1 https://doi.org/10.3847/1538-4357/add874
© 2025. The Author(s). Published by the American Astronomical Society.
OPEN ACCESS

The NANOGrav 15 yr Data Set: Search for Gravitational-wave Memory

Gabriella Agazie[1], Akash Anumarlapudi[1], Anne M. Archibald[2], Zaven Arzoumanian[3], Jeremy G. Baier[4], Paul T. Baker[5], Bence Bécsy[4], Laura Blecha[6], Adam Brazier[7,8], Paul R. Brook[9], Sarah Burke-Spolaor[10,11,68], Rand Burnette[4], J. Andrew Casey-Clyde[12], Maria Charisi[13], Shami Chatterjee[7], Tyler Cohen[14], James M. Cordes[7], Neil J. Cornish[15], Fronefield Crawford[16], H. Thankful Cromartie[17,69], Kathryn Crowter[18], Megan E. DeCesar[19,69], Paul B. Demorest[20], Heling Deng[4], Lankeswar Dey[10,11], Timothy Dolch[21,22], Elizabeth C. Ferrara[23,24,25], William Fiore[10,11], Emmanuel Fonseca[10,11], Gabriel E. Freedman[1], Emiko C. Gardiner[26], Nate Garver-Daniels[10,11], Peter A. Gentile[10,11], Kyle A. Gersbach[13], Joseph Glaser[10,11], Deborah C. Good[27], Kayhan Gültekin[28], Jeffrey S. Hazboun[4], Ross J. Jennings[10,11,70], Aaron D. Johnson[1,29], Megan L. Jones[1], David L. Kaplan[1], Luke Zoltan Kelley[26], Matthew Kerr[30], Joey S. Key[31], Nima Laal[4], Michael T. Lam[32,33,34], William G. Lamb[13], Bjorn Larsen[35], T. Joseph W. Lazio[36], Natalia Lewandowska[37], Tingting Liu[10,11], Duncan R. Lorimer[10,11], Jing Luo[38,71], Ryan S. Lynch[39], Chung-Pei Ma[26,40], Dustin R. Madison[41], Alexander McEwen[1], James W. McKee[42], Maura A. McLaughlin[10,11], Natasha McMann[13], Bradley W. Meyers[18,43], Patrick M. Meyers[29], Chiara M. F. Mingarelli[35], Andrea Mitridate[44], Priyamvada Natarajan[45,46], Cherry Ng[47], David J. Nice[48], Stella Koch Ocker[29,49], Ken D. Olum[50], Timothy T. Pennucci[51], Benetge B. P. Perera[52], Polina Petrov[13], Nihan S. Pol[53], Henri A. Radovan[54], Scott M. Ransom[55], Paul S. Ray[30], Jessie C. Runnoe[13], Alexander Saffer[55,70], Shashwat C. Sardesai[1], Ann Schmiedekamp[56], Carl Schmiedekamp[56], Kai Schmitz[57], Brent J. Shapiro-Albert[10,11,58], Xavier Siemens[1,4], Joseph Simon[59,72], Magdalena S. Siwek[60], Sophia V. Sosa Fiscella[33,34], Ingrid H. Stairs[18], Daniel R. Stinebring[61], Kevin Stovall[20], Jerry P. Sun[4], Abhimanyu Susobhanan[62], Joseph K. Swiggum[48,70], Jacob Taylor[4], Stephen R. Taylor[13], Jacob E. Turner[39], Caner Unal[63,64,65], Michele Vallisneri[29,36], Rutger van Haasteren[62], Sarah J. Vigeland[1], Haley M. Wahl[10,11], Caitlin A. Witt[66,67], David Wright[4], and Olivia Young[33,34]

[1] Center for Gravitation, Cosmology and Astrophysics, Department of Physics, University of Wisconsin-Milwaukee, P.O. Box 413, Milwaukee, WI 53201, USA
[2] Newcastle University, NE1 7RU, UK
[3] X-Ray Astrophysics Laboratory, NASA Goddard Space Flight Center, Code 662, Greenbelt, MD 20771, USA
[4] Department of Physics, Oregon State University, Corvallis, OR 97331, USA
[5] Department of Physics and Astronomy, Widener University, One University Place, Chester, PA 19013, USA
[6] Physics Department, University of Florida, Gainesville, FL 32611, USA
[7] Cornell Center for Astrophysics and Planetary Science and Department of Astronomy, Cornell University, Ithaca, NY 14853, USA
[8] Cornell Center for Advanced Computing, Cornell University, Ithaca, NY 14853, USA
[9] Institute for Gravitational Wave Astronomy and School of Physics and Astronomy, University of Birmingham, Edgbaston, Birmingham B15 2TT, UK
[10] Department of Physics and Astronomy, West Virginia University, P.O. Box 6315, Morgantown, WV 26506, USA
[11] Center for Gravitational Waves and Cosmology, West Virginia University, Chestnut Ridge Research Building, Morgantown, WV 26505, USA
[12] Department of Physics, University of Connecticut, 196 Auditorium Road, U-3046, Storrs, CT 06269-3046, USA
[13] Department of Physics and Astronomy, Vanderbilt University, 2301 Vanderbilt Place, Nashville, TN 37235, USA
[14] Department of Physics, New Mexico Institute of Mining and Technology, 801 Leroy Place, Socorro, NM 87801, USA
[15] Department of Physics, Montana State University, Bozeman, MT 59717, USA
[16] Department of Physics and Astronomy, Franklin & Marshall College, P.O. Box 3003, Lancaster, PA 17604, USA
[17] National Research Council Research Associate, National Academy of Sciences, Washington, DC 20001, USA
[18] Department of Physics and Astronomy, University of British Columbia, 6224 Agricultural Road, Vancouver, BC V6T 1Z1, Canada
[19] George Mason University, Fairfax, VA 22030, USA
[20] National Radio Astronomy Observatory, 1003 Lopezville Road, Socorro, NM 87801, USA
[21] Department of Physics, Hillsdale College, 33 E. College Street, Hillsdale, MI 49242, USA
[22] Eureka Scientific, 2452 Delmer Street, Suite 100, Oakland, CA 94602-3017, USA
[23] Department of Astronomy, University of Maryland, College Park, MD 20742, USA
[24] Center for Research and Exploration in Space Science and Technology, NASA/GSFC, Greenbelt, MD 20771, USA
[25] NASA Goddard Space Flight Center, Greenbelt, MD 20771, USA
[26] Department of Astronomy, University of California, Berkeley, 501 Campbell Hall #3411, Berkeley, CA 94720, USA
[27] Department of Physics and Astronomy, University of Montana, 32 Campus Drive, Missoula, MT 59812, USA
[28] Department of Astronomy and Astrophysics, University of Michigan, Ann Arbor, MI 48109, USA
[29] Division of Physics, Mathematics, and Astronomy, California Institute of Technology, Pasadena, CA 91125, USA
[30] Space Science Division, Naval Research Laboratory, Washington, DC 20375-5352, USA
[31] University of Washington Bothell, 18115 Campus Way NE, Bothell, WA 98011, USA
[32] SETI Institute, 339 N Bernardo Avenue Suite 200, Mountain View, CA 94043, USA
[33] School of Physics and Astronomy, Rochester Institute of Technology, Rochester, NY 14623, USA
[34] Laboratory for Multiwavelength Astrophysics, Rochester Institute of Technology, Rochester, NY 14623, USA
[35] Department of Physics, Yale University, New Haven, CT 06520, USA
[36] Jet Propulsion Laboratory, California Institute of Technology, 4800 Oak Grove Drive, Pasadena, CA 91109, USA
[37] Department of Physics and Astronomy, State University of New York at Oswego, Oswego, NY 13126, USA
[38] Department of Astronomy & Astrophysics, University of Toronto, 50 Saint George Street, Toronto, ON M5S 3H4, Canada
[39] Green Bank Observatory, P.O. Box 2, Green Bank, WV 24944, USA
[40] Department of Physics, University of California, Berkeley, CA 94720, USA
[41] Department of Physics, University of the Pacific, 3601 Pacific Avenue, Stockton, CA 95211, USA
[42] Department of Physics and Astronomy, Union College, Schenectady, NY 12308, USA
[43] International Centre for Radio Astronomy Research, Curtin University, Bentley, WA 6102, Australia

[44] Deutsches Elektronen-Synchrotron DESY, Notkestr. 85, 22607 Hamburg, Germany
[45] Department of Astronomy, Yale University, 52 Hillhouse Avenue, New Haven, CT 06511, USA
[46] Black Hole Initiative, Harvard University, 20 Garden Street, Cambridge, MA 02138, USA
[47] Dunlap Institute for Astronomy and Astrophysics, University of Toronto, 50 St. George Street, Toronto, ON M5S 3H4, Canada
[48] Department of Physics, Lafayette College, Easton, PA 18042, USA
[49] The Observatories of the Carnegie Institution for Science, Pasadena, CA 91101, USA
[50] Institute of Cosmology, Department of Physics and Astronomy, Tufts University, Medford, MA 02155, USA
[51] Institute of Physics and Astronomy, Eötvös Loránd University, Pázmány P. s. 1/A, 1117 Budapest, Hungary
[52] Arecibo Observatory, HC3 Box 53995, Arecibo, PR 00612, USA
[53] Department of Physics, Texas Tech University, Box 41051, Lubbock, TX 79409, USA
[54] Department of Physics, University of Puerto Rico, Mayagüez, PR 00681, USA
[55] National Radio Astronomy Observatory, 520 Edgemont Road, Charlottesville, VA 22903, USA
[56] Department of Physics, Penn State Abington, Abington, PA 19001, USA
[57] Institute for Theoretical Physics, University of Münster, 48149 Münster, Germany
[58] Giant Army, 915A 17th Ave, Seattle, WA 98122, USA
[59] Department of Astrophysical and Planetary Sciences, University of Colorado, Boulder, CO 80309, USA
[60] Center for Astrophysics, Harvard University, 60 Garden Street, Cambridge, MA 02138, USA
[61] Department of Physics and Astronomy, Oberlin College, Oberlin, OH 44074, USA
[62] Max-Planck-Institut für Gravitationsphysik (Albert-Einstein-Institut), Callinstrasse 38, D-30167, Hannover, Germany
[63] Department of Physics, Middle East Technical University, 06531 Ankara, Turkey
[64] Department of Physics, Ben-Gurion University of the Negev, Be'er Sheva 84105, Israel
[65] Feza Gursey Institute, Bogazici University, Kandilli, 34684, Istanbul, Turkey
[66] Center for Interdisciplinary Exploration and Research in Astrophysics (CIERA), Northwestern University, Evanston, IL 60208, USA
[67] Adler Planetarium, 1300 S. DuSable Lake Shore Drive, Chicago, IL 60605, USA
Received 2025 February 27; revised 2025 April 21; accepted 2025 May 12; published 2025 June 23

Abstract

We present the results of a search for nonlinear gravitational-wave (GW) memory in the NANOGrav 15 yr data set. We find no significant evidence for memory signals in the data set, with a maximum Bayes factor of 3.1 in favor of a model including memory. We therefore place upper limits on the strain of potential GW memory events as a function of sky location and observing epoch. We find upper limits that are not always more constraining than previous NANOGrav results. We show that it is likely due to the increase in common red noise between the 12.5 and 15 yr NANOGrav data sets.

Unified Astronomy Thesaurus concepts: Gravitational waves (678)

1. Introduction

Recent searches for gravitational waves (GWs) in Pulsar Timing Array (PTA) data have yielded strong evidence for the presence of a gravitational-wave background (G. Agazie et al. 2023b, 2023a; EPTA Collaboration et al. 2023a, 2023b; D. J. Reardon et al. 2023; H. Xu et al. 2023; A. Zic et al. 2023). With this new discovery, we are able to start probing the stochastic GW background produced in the nanohertz band (A. Afzal et al. 2023; G. Agazie et al. 2023c, 2023d, 2023e, 2023f), as well as other types of GW signals, including continuous waves (J. A. Ellis et al. 2012; Z. Arzoumanian et al. 2023; M. Falxa et al. 2023; EPTA Collaboration et al. 2024), bursts with memory (D. R. Madison et al. 2017; J. Sun et al. 2023; G. Agazie et al. 2024), and generic bursts (B. Bécsy & N. J. Cornish 2021; H. Deng et al. 2023; J. A. Taylor et al. 2025). In this paper, we present the results of our searches for GW memory in the NANOGrav 15 yr data set (G. Agazie et al. 2023a).

A PTA is a collection of millisecond pulsars (MSPs) with ultrastable rotational periods (D. R. Lorimer 2008). We can measure the times of arrival (TOAs) of the radio pulses from some of these MSPs to a precision of a few tens of nanoseconds for our best-timed pulsars. The pulse TOAs from an MSP depend on its period, spin-down rate, position, and motion across the sky, as well as orbital motion if the MSP is in a binary. Models that account for these effects can be used to predict the time at which each pulse is expected to arrive, and "timing residuals" are calculated by subtracting the model-predicted TOAs from the measured TOAs. GWs cause fluctuations in the TOAs that are correlated among MSPs (M. V. Sazhin 1978; S. Detweiler 1979; R. W. Hellings & G. S. Downs 1983).

We can search for GW memory responses in this data set from any theoretical source. Nonlinear GW memory is a constant shift in the gravitational metric due to violent GW-emitting events, such as mergers of supermassive black hole binaries (SMBHBs; D. Christodoulou 1991; A. G. Wiseman & C. M. Will 1991; K. S. Thorne 1992; M. Favata 2009). Events such as flybys of compact objects also source so-called linear GW memory effects (Y. B. Zel'dovich & A. G. Polnarev 1974). As a memory wave front passes the Earth or the pulsar, its effect is to redshift or blueshift the train of pulses traveling toward Earth. This appears to us as a sudden change in the rotational frequency of the pulsar, producing a linear drift in our timing residuals, which we will refer to as a ramp.

There have been several searches for GW memory in NANOGrav data sets (Z. Arzoumanian et al. 2015; K. Aggarwal et al. 2020; G. Agazie et al. 2024), as well as the Parkes PTA

[68] Resident at the U.S. Naval Research Laboratory, Washington, DC 20375, USA.
[69] Sloan Fellow.
[70] NANOGrav Physics Frontiers Center Postdoctoral Fellow.
[71] Deceased.
[72] NSF Astronomy and Astrophysics Postdoctoral Fellow.

Original content from this work may be used under the terms of the Creative Commons Attribution 4.0 licence. Any further distribution of this work must maintain attribution to the author(s) and the title of the work, journal citation and DOI.

(J. B. Wang et al. 2014), which have resulted in upper limits (ULs) on potential strains and event rates of memory events. There are also searches planned and ongoing for other ground- and space-based detectors like LISA, LIGO, VIRGO, and KAGRA (M. Favata 2009; P. Amaro-Seoane et al. 2017; O. M. Boersma et al. 2020; M. Hübner et al. 2020, 2021; A. M. Grant & D. A. Nichols 2023; S. Y. Cheung et al. 2024).

Here we report the results of a search for GW memory in the latest NANOGrav 15 yr data set (G. Agazie et al. 2023a). We find no compelling evidence for a GW memory event in this data set. A Bayesian model selection analysis only yielded a Bayes factor of BF = 3.1 in favor of a model including a GW memory event in the last 3 yr of the data set. Furthermore, GW memory bursts that occur late in a PTA data set are not credible since there are too few TOAs present after the event to convincingly rule out a noise transient. We also show that "hot spots" present in previous analyses are less significant in this data set (G. Agazie et al. 2024).

Having found no significant evidence for GW memory, we place updated ULs on GW memory strain and event rates. Following the procedure used in G. Agazie et al. (2024), we use single-pulsar likelihood lookup tables to expedite the calculation of global likelihoods (J. Sun et al. 2023). These ULs do not uniformly yield better constraints over the 12.5 yr data set results (G. Agazie et al. 2024). The latter are likely the effect of the increased common red noise signal we found in previous GW searches (G. Agazie et al. 2023c).

We begin Section 2 by reviewing the signal model for a GW memory event in PTA data. In Section 3, we detail the methods used to perform Bayesian model selection and compute ULs on the GW memory strain. Following that, in Section 4, we present the results of those searches and UL calculations. Finally, we present some conclusions in Section 5.

2. Signal

GW memory is a permanent change in the spacetime metric resulting from the anisotropic GW energy flux. In the context of PTA experiments, which measure the TOAs of radio pulses from pulsars, when a GW memory wave front passes over the Earth, we observe an apparent shift in the rotational frequencies of all pulsars in the data set. The sudden frequency change results in a constant excess or deficit of phase with each rotation of the pulsar, which in turn produces a "ramp"-shaped signature in the timing residuals.

We can write the residuals of a pulsar in the direction $\hat{\boldsymbol{p}}$ induced by a GW memory wave front passing Earth in the direction $\hat{\boldsymbol{k}}$ with a polarization ψ as

$$\delta t_{\rm mem}(t) = B(\hat{\boldsymbol{k}}, \hat{\boldsymbol{p}}, \psi) h_{\rm mem}(t). \tag{1}$$

Here, $B(\hat{\boldsymbol{k}}, \hat{\boldsymbol{p}}, \psi)$ accounts for the response of the Earth-pulsar system to a GW:

$$B(\hat{\boldsymbol{k}}, \hat{\boldsymbol{p}}, \psi) = \frac{1}{2}\cos(2\psi)(1 - \cos\alpha), \tag{2}$$

where α is the angle between $\hat{\boldsymbol{p}}$ and $\hat{\boldsymbol{k}}$. The time-dependent strain, $h_{\rm mem}(t)$, is given by

$$h_{\rm mem}(t) = h_0[(t - t_0)\Theta(t - t_0) - (t - t_i)\Theta(t - t_i)], \tag{3}$$

where t_0 is the time at which the memory wave front passes by the Earth, and $t_i = t_0 + (|\boldsymbol{p}|/c)[1 + \cos\alpha]$ is the time at which the wave front passes by the ith pulsar, and h_0 is the strain of the GW memory signal.

In the equation above, we often call the ramp term with t_0 the "Earth term," and the term with t_i the "pulsar term." The "Earth term" induces a ramp in the timing residuals when the GW wave front passes over the Earth and results in a change across all the pulsars. If a memory wave front passes over a pulsar, we get a "pulsar term" event. This causes that individual pulsar's apparent rotational frequency to change. However, because the change only occurs in one pulsar, and the time it takes that wave front to reach another pulsar vastly exceeds our data set length, it is difficult to distinguish a single pulsar GW memory event from some other transient effect, such as a pulsar glitch or noise transient (R. van Haasteren & Y. Levin 2010; J. M. Cordes & F. A. Jenet 2012). We therefore consider only the Earth term for all analyses but the event-rate ULs.

The full timing residuals for a single pulsar in our PTA are

$$\delta\boldsymbol{t} = \delta\boldsymbol{t}_{\rm mem} + M\boldsymbol{\epsilon} + \boldsymbol{n} + F\boldsymbol{a} + F_{\rm gw}\boldsymbol{a}_{\rm gw}. \tag{4}$$

In this equation, M is the design matrix that accounts for small errors in the pulsar timing model $\boldsymbol{\epsilon}$, and $\boldsymbol{n}$ is the white noise (WN) uncertainty. The pulsar-intrinsic red noise is modeled as a Fourier series with design matrix F and Fourier coefficient $\boldsymbol{a}$, while the common spatially uncorrelated red noise (CURN) process is modeled by the Fourier design matrix $F_{\rm GW}$ and coefficient $\boldsymbol{a}_{\rm GW}$. This is identical to the model used in G. Agazie et al. (2024).

We include both pulsar-intrinsic red noise and a common red noise since both have been shown to be present in these PTA data sets (Z. Arzoumanian et al. 2020; G. Agazie et al. 2023b) and model the red noise processes using power laws (E. S. Phinney 2001):

$$P_{\rm RN}(f) = A_{\rm RN}^2\left(\frac{f}{f_{1\ \rm yr}}\right)^{-\gamma}. \tag{5}$$

Here, $A_{\rm RN}$ is the red noise amplitude at the reference frequency $f_{1\ \rm yr}$, and γ is the spectral index.

Although the 15 yr data search has also revealed significant evidence that the common red noise process is due to GWs with Hellings–Downs (HD) correlations (R. W. Hellings & G. S. Downs 1983; G. Agazie et al. 2023b), we model it here as CURN because the methods used to make these analyses computationally efficient use a per-pulsar factorized likelihood (see Section 3 for details). Including interpulsar correlations in our model would require significantly more computational resources. Additionally, the HD coefficients are all less than or equal to 1/2, so they are, on average, small. This means that the terms along the diagonal of the pulsar covariance matrix are a factor of 6 larger than the off-diagonal terms, so modeling the common process as CURN still accounts for the majority of the effects of red noise.

3. Methods

The NANOGrav 15 yr data set consists of the pulse TOAs and timing models for 68 pulsars over a 15 yr timing baseline between 2004 July and 2020 August. For this paper, we exclude pulsar J0614−3329, which has a timing baseline shorter than 3 yr. A detailed description of the data set can be found in G. Agazie et al. (2023a).

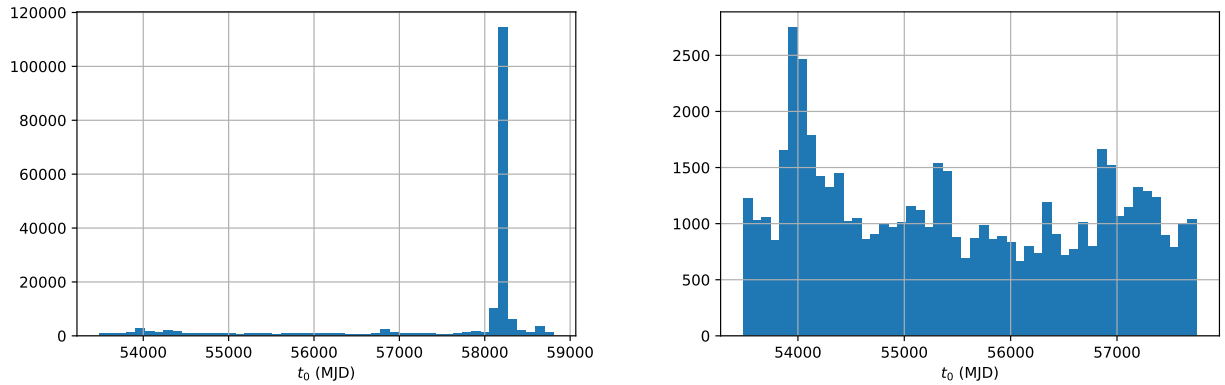

Figure 1. These histograms show the posterior distributions for the burst epoch (t_0) under different constraints on the Bayesian epoch priors. Left: the prior on t_0 is set to be the length of the data set with 270 days removed from either end to ignore low sensitivity around the data set edges (see Section 4.1). We see that there is one discernible event at 58200 MJD; however, this model is only favored by a Bayes factor of around 3 compared to the model without a GW memory event. Right: the prior is the same as the epoch prior used in the NANOGrav 12.5 yr search (G. Agazie et al. 2024). This provides more samples in the higher-sensitivity central times of the data set. This histogram shows only one notable, but small, feature, which occurs at the time of a sampling gap around 54000 MJD (G. Agazie et al. 2024). With these priors, the model including memory is actually disfavored by a factor of 1.22 when compared to a model including only red noise and no memory signal. These runs show no significant events over the span of the 15 yr data set.

To search for Earth-term GW memory, we use `enterprise` (J. A. Ellis et al. 2020) and `enterprise extensions` (S. R. Taylor et al. 2021) to perform model selection using Bayesian Markov Chain Monte Carlo product space sampling (B. P. Carlin & S. Chib 1995; S. J. Godsill 2001). In these searches, we use the likelihood as defined in Section 3 of Z. Arzoumanian et al. (2016), as well as log uniform priors on the pulsar-intrinsic red noise amplitude, CURN amplitude, and GW memory amplitude. For the GW memory epoch, we use uniform priors that exclude early and late times. Prior work in J. Sun et al. (2023) shows that the inclusion of early and late times can result in biased marginal posterior probability distributions of the GW strain amplitude.

To compute ULs, we begin by generating single-pulsar likelihood lookup tables. These lookup tables contain the likelihood for the GW strain marginalized over the pulsar-intrinsic red noise and CURN parameters. These can then be used to calculate the global likelihood because, as long as our noise covariance matrix is block diagonal, the likelihood can be factorized likelihood over pulsars. Specifically,

$$p(\delta t|\hat{\boldsymbol{k}}, \psi, t_0, h_0) = \prod_{i=1}^{N_{\rm psr}} p_i(\delta t|h_i, t_0), \tag{6}$$

where $h_i = B(\hat{\boldsymbol{k}}, \hat{\boldsymbol{p}}_i, \psi) \times h_0$. This improves the efficiency of calculations of the global Earth-term likelihoods by avoiding repeated expensive matrix inversions (see J. Sun et al. 2023 for more details)

When we numerically marginalize over the intrinsic red noise $\{A_{\rm IRN}, \gamma_{\rm IRN}\}$ and CURN $\{A_{\rm CURN}, \gamma_{\rm CURN}\}$ parameters for each pulsar, we use a log-uniform prior on the intrinsic red noise amplitude $\log_{10} A_{\rm IRN} \sim$ Uniform$(-16, -14)$ and a uniform prior on the spectral index $\gamma_{\rm IRN} \sim$ Uniform$(0, 7)$. For the CURN, we use the same prior for the amplitude as for the intrinsic red noise $\log_{10} A_{\rm CURN} \sim$ Uniform$(-16, -14)$. Rather than marginalizing over the spectral index, we fix it to the astrophysically predicted value for a background of GWs produced by SMBHBs $\gamma_{\rm CURN} = 13/3$. This simplifies the model without significantly affecting the overall CURN power, as we still marginalize over the amplitude, which is covariant with the spectral index. Further, as was shown in G. Agazie et al. (2024), the choice of spectral index does not change the resulting ULs significantly. This generates a noise-marginalized likelihood lookup table, with the only remaining non-sky location parameters being $\{h_0, t_B, \text{sign}(B(\hat{\boldsymbol{k}}, \hat{\boldsymbol{p}}, \psi))\}$.

4. Results

In this section, we present the results of Bayesian searches for GW memory events and ULs on the gravitational memory strain present in the NANOGrav 15 yr PTA.

4.1. Signal Search

We start with the Bayesian model selection analyses, where the two models being compared are (1) a model with Gaussian WN, per-pulsar red noise, CURN, and GW memory, and (2) a model that includes only WN, per-pulsar red noise, and CURN. We performed two analyses with slightly different priors on the burst epoch. The first prior excludes the first and last 270 days to avoid spurious GW events at the edges of our data set (G. Agazie et al. 2024). Events that are found early in the data set are nearly impossible to rule out because they are degenerate with the linear part of the quadratic fit. Events that are found very late in the data set have very few TOAs that support the "ramp"-shaped signature. The second prior constrains the burst epoch to the same time baseline as the NANOGrav 12.5 yr data set for comparisons with previous results.

The first analysis, which excludes 270 days from both ends of the data set, yields a Bayes factor of 3.1 ± 0.3 in favor of including a GW memory burst around $t_0 = 58{,}000$. As shown in the left histogram of Figure 1, this is the only significant potential event in the epoch posterior. For further information on how this event is localized in the sky and how it appears in pulsars, see the Appendix. Since this event occurs in the last 3 yr of the data set, where we have low sensitivity due to the lack of data to constrain the ramp, and the Bayes factor is not significant, there is no compelling evidence for a GW memory event.

The second analysis, which uses the same prior on the burst epoch as the NANOGrav 12.5 yr data set (shown in the right histogram of Figure 1), yields no evidence of any signals. This model selection run gave a Bayes factor of 1.22 ± 0.04, disfavoring the GW memory burst. The only visible peak,

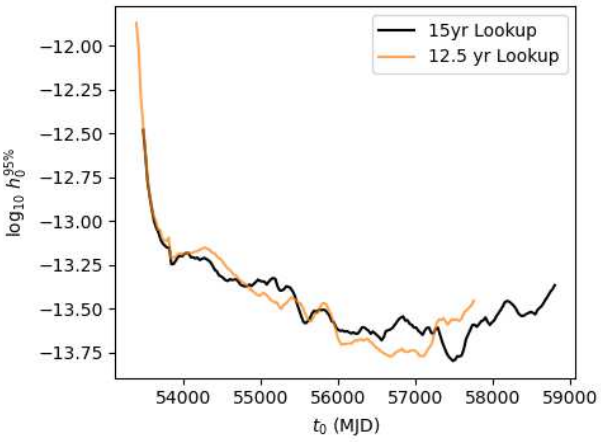

Figure 2. The 95% upper limits on the GW memory strain amplitude (h_0) for bursts at various epochs. Comparing the 15 and 12.5 yr upper limits from G. Agazie et al. (2024), we see improvements on the ends of the epoch time span and differences at central times due to the time baseline for the two timing models and the red noise levels in the two data sets.

around 54000 MJD, occurs near a well-known data gap at the beginning of the data set, which has been seen in the 11 and 12.5 yr searches (K. Aggarwal et al. 2020; G. Agazie et al. 2024). It is hard to constrain such a signal because of the quadratic subtraction done when we fit the timing model to the pulsar TOAs.

4.2. ULs

Having found no significant evidence of a detection, we move on to present ULs on GW memory events. We begin with strain-amplitude ULs versus burst epoch, which inform constraints on rates of GW memory events. Then we look at strain-amplitude ULs versus sky location. We compare all of these ULs to those computed in the NANOGrav 12.5 yr search for GW memory (G. Agazie et al. 2024). Finally, we also provide some context for the trends we see with regard to the red noise levels in the data sets.

4.2.1. UL versus Epoch

Figure 2 shows the strain UL as a function of burst epoch marginalized over sky location and polarization. The burst epoch is sampled using a uniform prior, while the sky location and polarization are marginalized by taking an equal number of samples from every source orientation bin to avoid bias from the least sensitive sky locations. We also use the burst-epoch ULs to calculate ULs on the merger rates of SMBHBs in Figure 3. We present these new ULs and compare them with our previous 12.5 yr data set results.

The 15 yr ULs deviate from the 12.5 yr ULs in a number of ways. Starting with the strain ULs, there is some improvement at early epochs in the 15 yr results. However, near the middle of the data set, there is a loss of sensitivity before our highest sensitivity around 57600 MJD. We believe this to be the result of the quadratic subtraction necessary for our timing model, which reduces sensitivity near the center of each pulsar's timing baselines (R. van Haasteren & Y. Levin 2010; J. M. Cordes & F. A. Jenet 2012). Now that we have more pulsars with data in the most recent 3 yr, the sensitivity loss from quadratic subtraction that occurs in the middle of a data set has shifted to a later period in the data set. The small changes in our recovered CURN parameters also have a significant effect on the recovered ULs. See Section 4.2.3 for further discussion of this effect.

We can convert these strain ULs into event-rate ULs as well. We do this by counting the number of samples that fall below a given strain amplitude, calculating what portion of the total timing baseline is using the time spacing between samples, and then taking the reciprocal of the cumulative time to give the event-rate constraint for that strain amplitude. The event-rate ULs also show some differences from the 12.5 yr data set. At high strains, we see more constrained event-rate ULs for both the Earth and pulsar terms, while at lower strains, the event rate is less constrained when considering the pulsar term. These low-strain event limits are dominated by our longest-timed pulsars, which are affected the most significantly by the change in red noise amplitude between data sets.

4.2.2. UL versus Sky Location

We also present the epoch-marginalized ULs as a function of source sky location. These ULs show how sensitivity varies across the sky. To compute these ULs, we marginalize over a specified range of GW memory epochs while sampling over a grid of sky locations. This is displayed in the top plot of Figure 4. As expected, when using the last 3 yr of data from the 15 yr data set, we see the lowest ULs in the most densely populated regions of the sky. However, the ULs still do not reach below $h_0 = 10^{-14}$ in these regions.

Figure 4 shows the difference in ULs on GW strain between the 15 yr and the 12.5 yr analyses. Both are plots averaged over the last 3 yr period of the 12.5 yr data set, which was the period analyzed in G. Agazie et al. (2024), and allows the direct comparison of results. We see that over most of the sky, there is an improvement in these ULs in the 15 yr search. In other words, the 15 yr ULs are lower in most parts of the sky. This is consistent with the differences we see over these times in the UL versus epoch results above, as epochs near the end of our data set have decreased ULs for the 15 yr compared to the 12.5 yr results. In some of that region, it is higher for the 15 yr, which is still consistent, as the differences between the two results are not large.

4.2.3. Signal-to-noise Scaling Expectation

Some of the above results are surprising, most notably the loss of sensitivity between the MJDs of 56000 and 57000 seen in Figure 2. In order to better understand how red noise may affect GW memory sensitivity, we also performed a simple test of how GW memory signal-to-noise ratio (SNR) changes between the 12.5 and 15 yr memory searches. This test estimates how much of an increase in GW memory event detectability we expect to see given the extensions of our data set, as well as the shifts we have seen in the amplitude of the GW background between these two data sets. To do this, we used a simple simulated data set that includes a Gaussian WN process, CURN, and GW memory event that starts $t_B = 4$ yr into the data set with a strain of $h_0 = 10^{-14.5}$. The WN level is set to 0.5 μs for all pulsars. We fix the spectral index of the CURN to $\gamma = \frac{13}{3}$ and compare the resulting time evolution of the SNR while fixing the amplitude of the CURN to the maximum a posteriori values from the results of the NANOGrav 15 yr ($A = 2.4 \times 10^{-15}$) and 12.5 yr ($A = 1.9 \times 10^{-15}$) searches for a

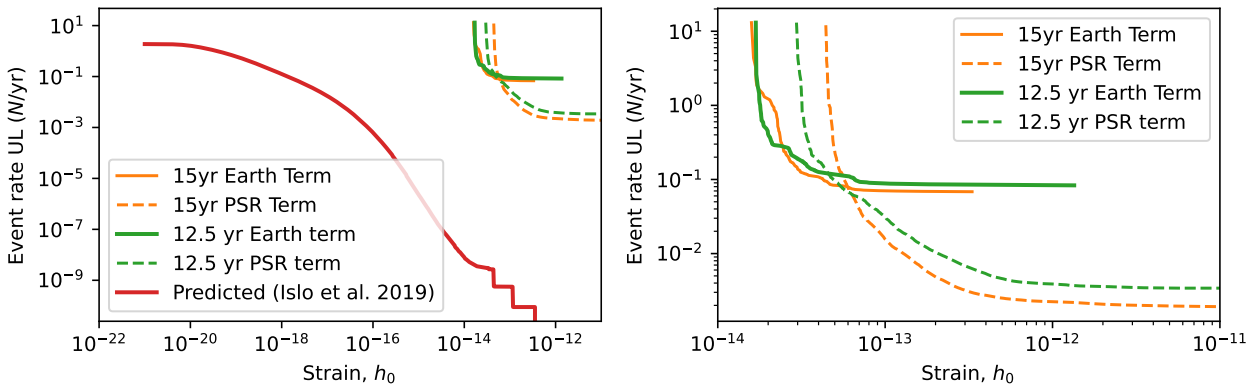

Figure 3. Upper limits on the GW memory event rate in the combined individual pulsar (PSR) terms, as well as the Earth term. These are presented vs. GW memory strain (h_0), with the (right) plot presenting the same data zoomed in to a strain range of 10^{-14}–10^{-11}.

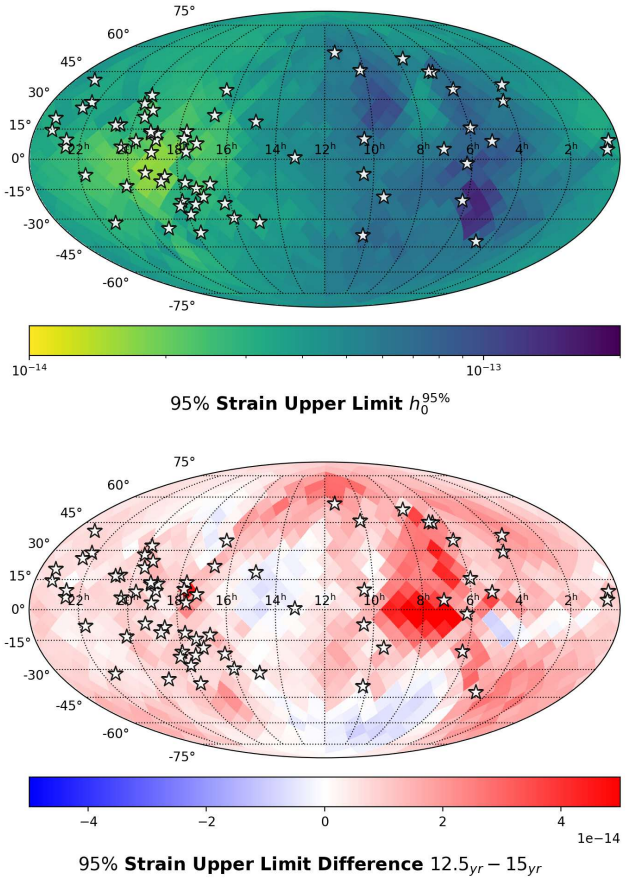

Figure 4. The top plot is an upper limit on strain amplitude across the sky, averaged over the final 3 yr of the 15 yr NANOGrav data set. The bottom plot is the difference in upper limits between the 15 and 12.5 yr searches during the last 3 yr of the 12.5 yr data set.

stochastic GW background. We calculate these SNRs by taking the inner product of the post-timing-model-fit GW memory signal with itself using the R-matrix formalism and the noise covariance matrix as described in S. J. Chamberlin et al. (2015).

The results are shown in Figure 5, where we display the mean SNR and 1σ uncertainty in the SNR for 100 realizations of a data set including 40 pulsars, with CURN parameters and timing baseline matching with either the 15 yr or 12.5 yr data set. This demonstrates that having a longer timing baseline does reduce the variance in the SNR and provides some increase in SNR value on the timescales of these data sets

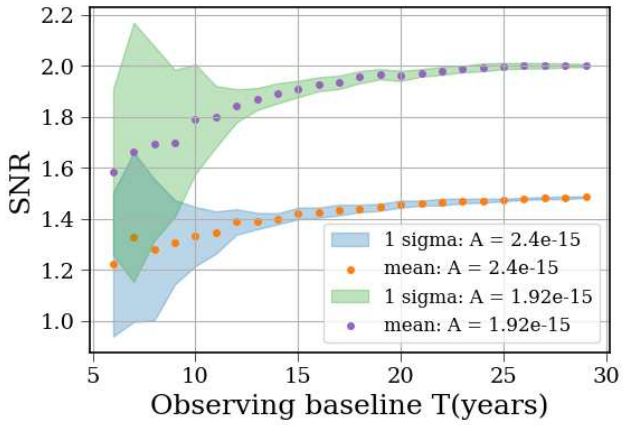

Figure 5. SNR of a GW memory signal given two potential CURN amplitudes and over a variety of pulsar timing baselines. The green section with red dots has a CURN consistent with the 12.5 yr data set, while the blue section with orange dots has a CURN consistent with the 15 yr data set. Both the mean and 1σ SNRs are calculated over 100 realizations of the noise.

(5–15 yr). However, the difference in the CURN amplitude between these two data sets also has a significant impact on the SNR. The larger CURN amplitude found in the 15 yr data set reduces the SNR by approximately 25% over the course of a long observation baseline.

This simple test gives us insight into why the ULs presented in this paper are worse at some epochs. The increased amplitude of the red noise background in our data reduces the significance of GW memory signals. We plan to perform a more extensive evaluation of the GW memory signal scaling in PTA data in the future, including an update to the detection prospect work presented in K. Islo et al. (2019).

5. Conclusion

We performed a search for GW memory events in NANOGrav's 15 yr data set and found no significant evidence in favor of such events. The only discernible event occurred near the end of the data set, around an MJD of 58200, as shown in Figure 1. For this event, model selection yields an insignificant Bayes factor of 3.1 in favor of the model with GW memory. As this event occurs late in the data set, where there is not enough data remaining to well constrain GW memory buildup, we believe this to be a spurious event. We will need future data sets to definitively rule this event out.

This could be due to the fact that there is not enough data remaining to build up the GW memory significance after the time the event occurs. Future data sets will be able to determine if this event is spurious.

Having found no significant events, we proceed to set new ULs on GW memory. Overall, in the early times of sky-averaged ULs (Figure 2), the earth term and high-strain pulsar term event-rate ULs (Figure 3), and the epoch-averaged UL sky maps (Figure 4), we see improvements in these ULs over the previous 12.5 yr search. However, these improvements are not uniform, and the strain ULs in central times of the 15 yr data set are less constraining. We also see these constraints weaken for low-strain pulsar term event-rate ULs. This loss of sensitivity is due to the increased CURN amplitude recovered in the 15 yr data set compared with the 12.5 yr data set, as well as the effects of quadratic subtraction (J. M. Cordes & F. A. Jenet 2012) compounded over the various pulsar timing baselines, which have changed between the data sets.

While we do not expect our new constraints for the SMBHB population to be astrophysically interesting (see Figure 3), our limits apply to all astrophysical and cosmological sources of GW memory. Because all GW-emitting events act as sources for GW memory, these searches will continue to be an important catchall for constraining more exotic GW sources.

Acknowledgments

The work contained herein has been carried out by the NANOGrav collaboration, which receives support from the National Science Foundation (NSF) Physics Frontier Center award Nos. 1430284 and 2020265, the Gordon and Betty Moore Foundation, NSF AccelNet award No. 2114721, an NSERC Discovery Grant, and CIFAR. The Arecibo Observatory is a facility of the NSF operated under cooperative agreement (AST-1744119) by the University of Central Florida (UCF) in alliance with Universidad Ana G. Méndez (UAGM) and Yang Enterprises (YEI), Inc. The Green Bank Observatory is a facility of the NSF operated under cooperative agreement by Associated Universities, Inc. L.B. acknowledges support from the National Science Foundation under award AST-1909933 and from the Research Corporation for Science Advancement under Cottrell Scholar Award No. 27553. P.R.B. is supported by the Science and Technology Facilities Council, grant No. ST/W000946/1. S.B. gratefully acknowledges the support of a Sloan Fellowship, and the support of NSF under award #1815664. The work of R.B., N. La., X.S., J.P.S., J.T., and D.W. is partly supported by the George and Hannah Bolinger Memorial Fund in the College of Science at Oregon State University. M.C., P.P., and S.R.T. acknowledge support from NSF AST-2007993. M.C. was supported by the Vanderbilt Initiative in Data Intensive Astrophysics (VIDA) Fellowship. Support for this work was provided by the NSF through the Grote Reber Fellowship Program administered by Associated Universities, Inc. /National Radio Astronomy Observatory. Pulsar research at UBC is supported by an NSERC Discovery Grant and by CIFAR. K.C. is supported by a UBC Four Year Fellowship (6456). M.E.D. acknowledges support from the Naval Research Laboratory by NASA under contract S-15633Y. T. D. and M.T.L. were supported by an NSF Astronomy and Astrophysics Grant (AAG) award No. 2009468 during this work. E.C.F. is supported by NASA under award No. 80GSFC24M0006. G.E.F., S.C.S., and S.J.V. are supported by NSF award PHY-2011772. K.A.G. and S.R.T. acknowledge support from an NSF CAREER award #2146016. A.D.J. and M.V. acknowledge support from the Caltech and Jet Propulsion Laboratory President's and Director's Research and Development Fund. A.D.J. acknowledges support from the Sloan Foundation. N.La. acknowledges the support from Larry W. Martin and Joyce B. O'Neill Endowed Fellowship in the College of Science at Oregon State University. Part of this research was carried out at the Jet Propulsion Laboratory, California Institute of Technology, under a contract with the National Aeronautics and Space Administration (80NM0018D0004). D.R.L. and M.A.M. are supported by NSF #1458952. M.A.M. is supported by NSF #2009425. C.M.F.M. was supported in part by the National Science Foundation under grants No. NSF PHY-1748958 and AST-2106552. A.Mi. is supported by the Deutsche Forschungsgemeinschaft under Germany's Excellence Strategy - EXC 2121 Quantum Universe - 390833306. The Dunlap Institute is funded by an endowment established by the David Dunlap family and the University of Toronto. P.N. acknowledges support from the BHI, funded by grants from the John Templeton Foundation and the Gordon and Betty Moore Foundation. K.D.O. was supported in part by NSF grant No. 2207267. T.T.P. acknowledges support from the Extragalactic Astrophysics Research Group at Eötvös Loránd University, funded by the Eötvös Loránd Research Network (ELKH), which was used during the development of this research. H.A. R. is supported by NSF Partnerships for Research and Education in Physics (PREP) award No. 2216793. S.M.R. and I.H.S. are CIFAR Fellows. Portions of this work performed at NRL were supported by ONR 6.1 basic research funding. J.D.R. also acknowledges support from start-up funds from Texas Tech University. J.S. is supported by an NSF Astronomy and Astrophysics Postdoctoral Fellowship under award AST-2202388, and acknowledges previous support by the NSF under award 1847938. C.U. acknowledges support from BGU (Kreitman fellowship), and the Council for Higher Education and Israel Academy of Sciences and Humanities (Excellence fellowship). C.A.W. acknowledges support from CIERA, the Adler Planetarium, and the Brinson Foundation through a CIERA-Adler postdoctoral fellowship. O.Y. is supported by the National Science Foundation Graduate Research Fellowship under grant No. DGE-2139292.

We thank the anonymous referee for careful review of our paper.

Author Contributions

We present the author list in alphabetical order in recognition that this paper is the result of the decades-long work of many people in the NANOGrav Collaboration. All authors contributed to the activities of the NANOGrav Collaboration, leading to the work presented here, and reviewed the manuscript, text, and figures prior to the paper submission. Specific author contributions are as follows. G.A., A.A., A.M.A., Z.A., P.T.B., P.R.B., H.T.C., K.C., M.E.D., P.B.D., T.D., E.C.F., W.F., E.F., G.E.F., N.G., P.A.G., J.G., D.C.G., J.S.H., R.J.J., M.L.J., D.L.K., M.K., M.T.L., D.R.L., J.L., R.S.L., A.M., M.A.M., N.M., B.W.M., C. N., D.J.N., P.N., T.T.P., B.B.P.P., N.S.P., H.A.R., S.M.R., P.S. R., A.S., C.S., B.J.S., I.H.S., K.S., A.S., J.K.S., and H.M.W. contributed through a combination of observations, arrival time calculations, data checks and refinements, and timing model development and analysis; additional specific contributions to

the data set are summarized in G. Agazie et al. (2023a). R.B. ran the Bayesian detection and upper limit analysis and wrote the bulk of the paper. J.S. assisted in paper writing, analysis, and code debugging, and ran simulations for SNR scaling tests. B. B., J.S.H., J.T., and X.S. provided guidance on searches and analysis.

Appendix
Pulsar Localization of the GW Memory Event

In this appendix, we show sky localization and pulsar responses of the most distinct event in our model selection analysis, occurring at 58200 MJD. We limit our analysis to samples with a GW memory epoch (t_0) in the range 58100–58300 MJD. The mode values of the sky location and polarization parameters from these constrained posteriors are $\theta = 2.9$, $\phi = 3.6$, and $\psi = 0.47$ radians. In Figure 6, we plot the normalized antenna response of the GW memory event across the sky, and can see that there are a few pulsars that sit in the polarization lobes. We plotted the residuals along with the GW memory delays for the six pulsars with the largest antenna pattern response, which are pulsars J0437−4715, J0931−1902, J1012−4235, J1455−3330, J1600−3053, and J2124−3358, marked with the larger red stars in Figure 6.

For these six pulsars, we plot the residuals post-timing-model fit, along with the GW memory delay, in Figure 7. All of these pulsars appear to be WN dominated, with the GW memory delay well below the WN floor. This is consistent with this event being spurious.

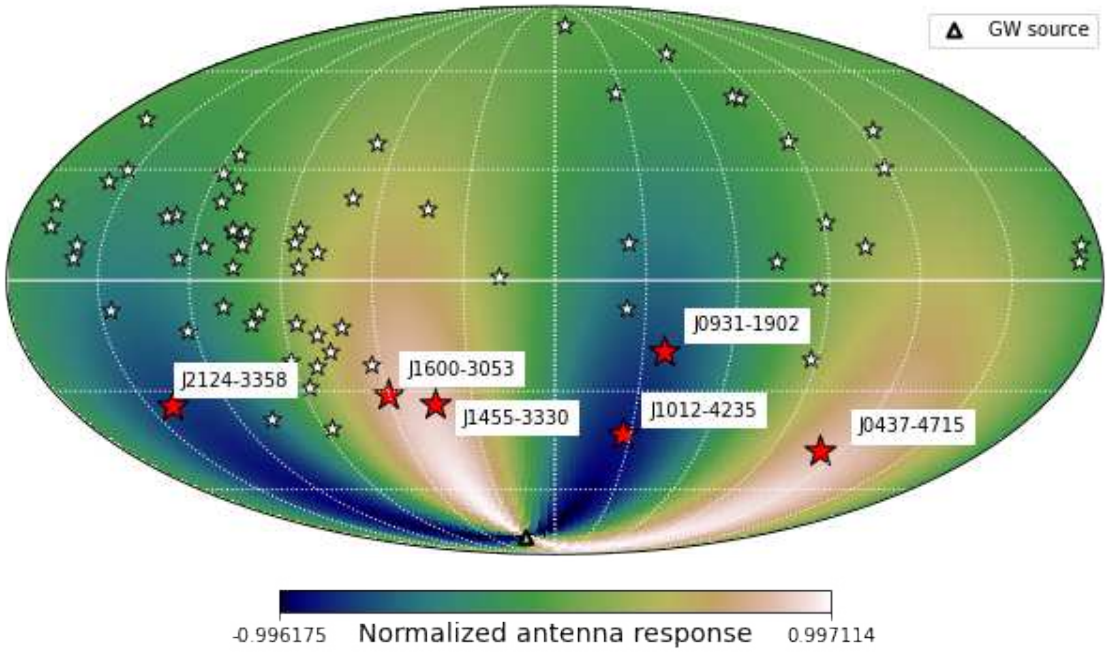

Figure 6. Plot of the normalized antenna response for the low-significance GW memory burst that appears to be present around $t_0 = 58{,}200$. We also show the locations of the pulsars from the NANOGrav 15 yr data set, with the six pulsars nearest the burst lobes labeled and indicated with larger red stars.

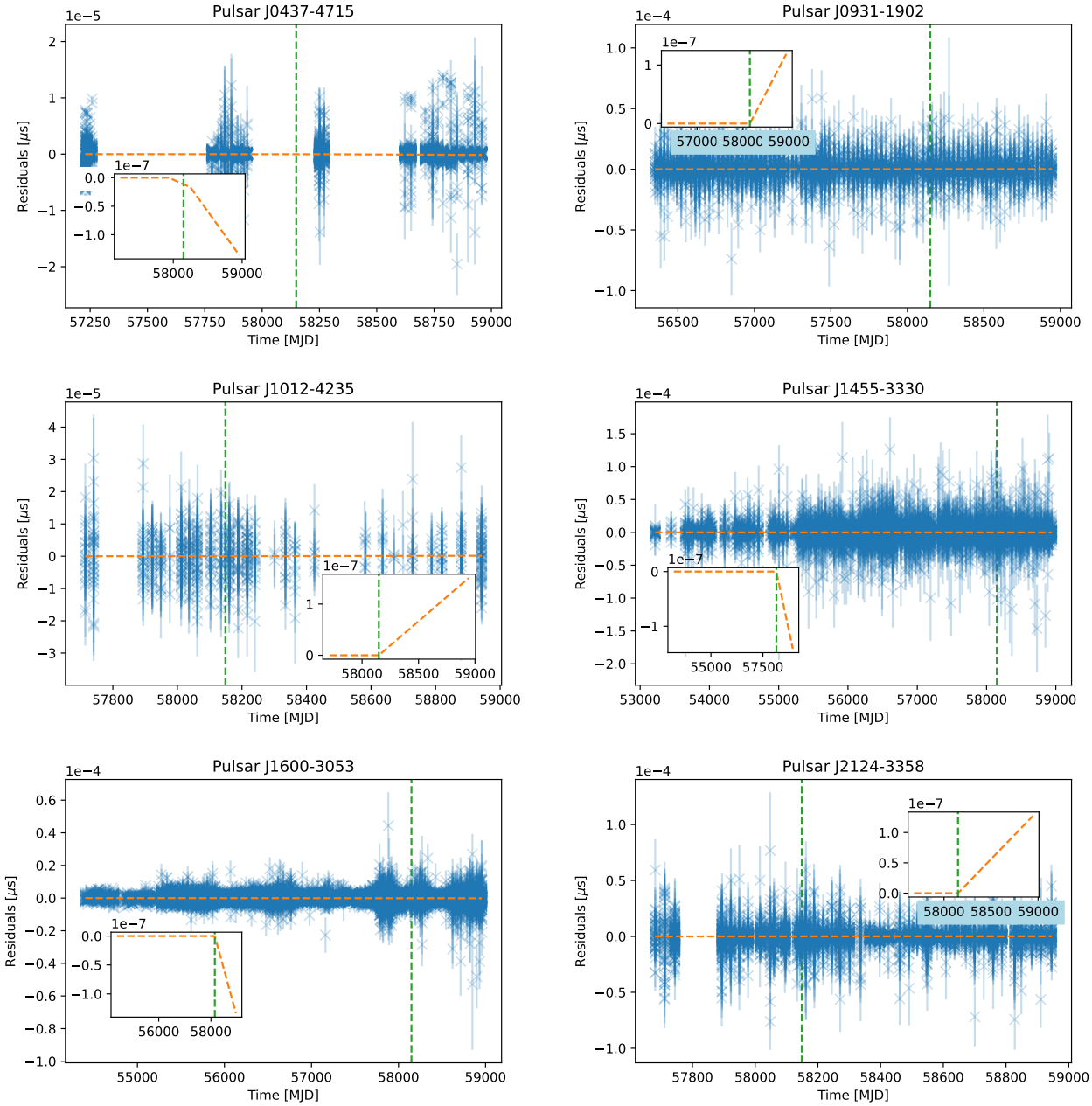

Figure 7. Plots of the timing residuals for six pulsars in the NANOGrav 15 yr data set, along with GW memory signal delays and epoch locations for each pulsar. The blue crosshair markers are the residuals with error bars, the vertical green lines indicate the GW memory epoch (t_0), and the orange dashed lines are the GW memory delays in the respective pulsars. The subplots display the same data on the same axis but exclude the residuals so that the scale of the GW memory delays is more visible. The memory signal is at least 2 orders of magnitude below the white noise levels in all these pulsars.

ORCID iDs

Gabriella Agazie https://orcid.org/0000-0001-5134-3925
Akash Anumarlapudi https://orcid.org/0000-0002-8935-9882
Anne M. Archibald https://orcid.org/0000-0003-0638-3340
Zaven Arzoumanian https://orcid.org/0009-0008-6187-8753
Jeremy G. Baier https://orcid.org/0000-0002-4972-1525
Paul T. Baker https://orcid.org/0000-0003-2745-753X
Bence Bécsy https://orcid.org/0000-0003-0909-5563
Laura Blecha https://orcid.org/0000-0002-2183-1087
Adam Brazier https://orcid.org/0000-0001-6341-7178
Paul R. Brook https://orcid.org/0000-0003-3053-6538
Sarah Burke-Spolaor https://orcid.org/0000-0003-4052-7838
Rand Burnette https://orcid.org/0009-0008-3649-0618
J. Andrew Casey-Clyde https://orcid.org/0000-0002-5557-4007
Maria Charisi https://orcid.org/0000-0003-3579-2522
Shami Chatterjee https://orcid.org/0000-0002-2878-1502
Tyler Cohen https://orcid.org/0000-0001-7587-5483
James M. Cordes https://orcid.org/0000-0002-4049-1882
Neil J. Cornish https://orcid.org/0000-0002-7435-0869
Fronefield Crawford https://orcid.org/0000-0002-2578-0360
H. Thankful Cromartie https://orcid.org/0000-0002-6039-692X
Kathryn Crowter https://orcid.org/0000-0002-1529-5169
Megan E. DeCesar https://orcid.org/0000-0002-2185-1790
Paul B. Demorest https://orcid.org/0000-0002-6664-965X
Lankeswar Dey https://orcid.org/0000-0002-2554-0674
Timothy Dolch https://orcid.org/0000-0001-8885-6388
Elizabeth C. Ferrara https://orcid.org/0000-0001-7828-7708
William Fiore https://orcid.org/0000-0001-5645-5336
Emmanuel Fonseca https://orcid.org/0000-0001-8384-5049

Gabriel E. Freedman https://orcid.org/0000-0001-7624-4616
Emiko C. Gardiner https://orcid.org/0000-0002-8857-613X
Nate Garver-Daniels https://orcid.org/0000-0001-6166-9646
Peter A. Gentile https://orcid.org/0000-0001-8158-683X
Joseph Glaser https://orcid.org/0000-0003-4090-9780
Deborah C. Good https://orcid.org/0000-0003-1884-348X
Kayhan Gültekin https://orcid.org/0000-0002-1146-0198
Jeffrey S. Hazboun https://orcid.org/0000-0003-2742-3321
Ross J. Jennings https://orcid.org/0000-0003-1082-2342
Aaron D. Johnson https://orcid.org/0000-0002-7445-8423
Megan L. Jones https://orcid.org/0000-0001-6607-3710
David L. Kaplan https://orcid.org/0000-0001-6295-2881
Luke Zoltan Kelley https://orcid.org/0000-0002-6625-6450
Matthew Kerr https://orcid.org/0000-0002-0893-4073
Joey S. Key https://orcid.org/0000-0003-0123-7600
Nima Laal https://orcid.org/0000-0002-9197-7604
Michael T. Lam https://orcid.org/0000-0003-0721-651X
William G. Lamb https://orcid.org/0000-0003-1096-4156
Bjorn Larsen https://orcid.org/0000-0001-6436-8216
Natalia Lewandowska https://orcid.org/0000-0003-0771-6581
Tingting Liu https://orcid.org/0000-0001-5766-4287
Duncan R. Lorimer https://orcid.org/0000-0003-1301-966X
Jing Luo https://orcid.org/0000-0001-5373-5914
Ryan S. Lynch https://orcid.org/0000-0001-5229-7430
Chung-Pei Ma https://orcid.org/0000-0002-4430-102X
Dustin R. Madison https://orcid.org/0000-0003-2285-0404
Alexander McEwen https://orcid.org/0000-0001-5481-7559
James W. McKee https://orcid.org/0000-0002-2885-8485
Maura A. McLaughlin https://orcid.org/0000-0001-7697-7422
Natasha McMann https://orcid.org/0000-0002-4642-1260
Bradley W. Meyers https://orcid.org/0000-0001-8845-1225
Patrick M. Meyers https://orcid.org/0000-0002-2689-0190
Chiara M. F. Mingarelli https://orcid.org/0000-0002-4307-1322
Andrea Mitridate https://orcid.org/0000-0003-2898-5844
Priyamvada Natarajan https://orcid.org/0000-0002-5554-8896
Cherry Ng https://orcid.org/0000-0002-3616-5160
David J. Nice https://orcid.org/0000-0002-6709-2566
Stella Koch Ocker https://orcid.org/0000-0002-4941-5333
Ken D. Olum https://orcid.org/0000-0002-2027-3714
Timothy T. Pennucci https://orcid.org/0000-0001-5465-2889
Benetge B. P. Perera https://orcid.org/0000-0002-8509-5947
Polina Petrov https://orcid.org/0000-0001-5681-4319
Nihan S. Pol https://orcid.org/0000-0002-8826-1285
Henri A. Radovan https://orcid.org/0000-0002-2074-4360
Scott M. Ransom https://orcid.org/0000-0001-5799-9714
Paul S. Ray https://orcid.org/0000-0002-5297-5278
Jessie C. Runnoe https://orcid.org/0000-0001-8557-2822
Alexander Saffer https://orcid.org/0000-0001-7832-9066
Shashwat C. Sardesai https://orcid.org/0009-0006-5476-3603
Ann Schmiedekamp https://orcid.org/0000-0003-4391-936X
Carl Schmiedekamp https://orcid.org/0000-0002-1283-2184
Kai Schmitz https://orcid.org/0000-0003-2807-6472
Brent J. Shapiro-Albert https://orcid.org/0000-0002-7283-1124
Xavier Siemens https://orcid.org/0000-0002-7778-2990
Joseph Simon https://orcid.org/0000-0003-1407-6607
Magdalena S. Siwek https://orcid.org/0000-0002-1530-9778
Sophia V. Sosa Fiscella https://orcid.org/0000-0002-5176-2924
Ingrid H. Stairs https://orcid.org/0000-0001-9784-8670
Daniel R. Stinebring https://orcid.org/0000-0002-1797-3277
Kevin Stovall https://orcid.org/0000-0002-7261-594X
Jerry P. Sun https://orcid.org/0000-0002-7933-493X
Abhimanyu Susobhanan https://orcid.org/0000-0002-2820-0931
Joseph K. Swiggum https://orcid.org/0000-0002-1075-3837
Jacob Taylor https://orcid.org/0000-0001-9118-5589
Stephen R. Taylor https://orcid.org/0000-0001-8217-1599
Jacob E. Turner https://orcid.org/0000-0002-2451-7288
Caner Unal https://orcid.org/0000-0001-8800-0192
Michele Vallisneri https://orcid.org/0000-0002-4162-0033
Rutger van Haasteren https://orcid.org/0000-0002-6428-2620
Sarah J. Vigeland https://orcid.org/0000-0003-4700-9072
Haley M. Wahl https://orcid.org/0000-0001-9678-0299
Caitlin A. Witt https://orcid.org/0000-0002-6020-9274
David Wright https://orcid.org/0000-0003-1562-4679
Olivia Young https://orcid.org/0000-0002-0883-0688

References

Afzal, A., Agazie, G., Anumarlapudi, A., et al. 2023, ApJL, 951, L11
Agazie, G., Alam, M. F., Anumarlapudi, A., et al. 2023a, ApJL, 951, L9
Agazie, G., Anumarlapudi, A., Archibald, A. M., et al. 2023b, ApJL, 951, L8
Agazie, G., Anumarlapudi, A., Archibald, A. M., et al. 2023c, ApJL, 951, L50
Agazie, G., Anumarlapudi, A., Archibald, A. M., et al. 2023d, ApJL, 951, L10
Agazie, G., Anumarlapudi, A., Archibald, A. M., et al. 2023e, ApJL, 952, L37
Agazie, G., Anumarlapudi, A., Archibald, A. M., et al. 2023f, ApJL, 956, L3
Agazie, G., Arzoumanian, Z., Baker, P. T., et al. 2024, ApJ, 963, 61
Aggarwal, K., Arzoumanian, Z., Baker, P. T., et al. 2020, ApJ, 889, 38
Amaro-Seoane, P., Audley, H., Babak, S., et al. 2017, arXiv:1702.00786
Arzoumanian, Z., Baker, P. T., Blecha, L., et al. 2023, ApJL, 951, L28
Arzoumanian, Z., Baker, P. T., Blumer, H., et al. 2020, ApJL, 905, L34
Arzoumanian, Z., Brazier, A., Burke-Spolaor, S., et al. 2015, ApJ, 810, 150
Arzoumanian, Z., Brazier, A., Burke-Spolaor, S., et al. 2016, ApJ, 821, 13
Bécsy, B., & Cornish, N. J. 2021, CQGra, 38, 095012
Boersma, O. M., Nichols, D. A., & Schmidt, P. 2020, PhRvD, 101, 083026
Carlin, B. P., & Chib, S. 1995, J. R. Stat. Soc.: Ser. B (Methodol.), 57, 473
Chamberlin, S. J., Creighton, J. D., Siemens, X., et al. 2015, PhRvD, 91
Cheung, S. Y., Lasky, P. D., & Thrane, E. 2024, CQGra, 41, 115010
Christodoulou, D. 1991, PhRvL, 67, 1486
Cordes, J. M., & Jenet, F. A. 2012, ApJ, 752, 54
Deng, H., Bécsy, B., Siemens, X., Cornish, N. J., & Madison, D. R. 2023, PhRvD, 108, 102007
Detweiler, S. 1979, ApJ, 234, 1100
Ellis, J. A., Siemens, X., & Creighton, J. D. E. 2012, ApJ, 756, 175
Ellis, J. A., Vallisneri, M., Taylor, S. R., & Baker, P. T. 2020, ENTERPRISE: Enhanced Numerical Toolbox Enabling a Robust PulsaR Inference SuitE, v3.3.3, Zenodo, doi:10.5281/ZENODO.4059815
EPTA Collaboration, Antoniadis, J., Babak, S., et al. 2023a, A&A, 678, A48
EPTA Collaboration, InPTA Collaboration, Antoniadis, J., et al. 2023b, A&A, 678, A50
EPTA Collaboration, InPTA Collaboration, Antoniadis, J., et al. 2024, A&A, 690, A118
Falxa, M., Babak, S., Baker, P. T., et al. 2023, MNRAS, 521, 5077
Favata, M. 2009, ApJ, 696, L159
Godsill, S. J. 2001, J. Comput. Graphical Stat., 10, 230
Grant, A. M., & Nichols, D. A. 2023, PhRvD, 107
Hellings, R. W., & Downs, G. S. 1983, ApJ, 265, L39
Hübner, M., Lasky, P., & Thrane, E. 2021, PhRvD, 104, 023004
Hübner, M., Talbot, C., Lasky, P. D., & Thrane, E. 2020, PhRvD, 101, 023011
Islo, K., Simon, J., Burke-Spolaor, S., & Siemens, X. 2019, arXiv:1906.11936
Lorimer, D. R. 2008, LRR, 11, 8
Madison, D. R., Chernoff, D. F., & Cordes, J. M. 2017, PhRvD, 96, 123016
Phinney, E. S. 2001, arXiv:astro-ph/0108028
Reardon, D. J., Zic, A., Shannon, R. M., et al. 2023, ApJL, 951, L6
Sazhin, M. V. 1978, SvA, 22, 36
Sun, J., Baker, P. T., Johnson, A. D., Madison, D. R., & Siemens, X. 2023, ApJ, 951, 121
Taylor, J. A., Burnette, R., Bécsy, B., & Cornish, N. J. 2025, PhRvD, 111, 022006
Taylor, S. R., Baker, P. T., Hazboun, J. S., Simon, J., & Vigeland, S. J. 2021, enterprise_extensions, v2.4.2, GitHub, https://github.com/nanograv/enterprise_extensions
Thorne, K. S. 1992, PhRvD, 45, 520
van Haasteren, R., & Levin, Y. 2010, MNRAS, 401, 2372
Wang, J. B., Hobbs, G., Coles, W., et al. 2014, MNRAS, 446, 1657
Wiseman, A. G., & Will, C. M. 1991, PhRvD, 44, R2945
Xu, H., Chen, S., Guo, Y., et al. 2023, RAA, 23, 075024
Zel'dovich, Y. B., & Polnarev, A. G. 1974, SvA, 18, 17
Zic, A., Reardon, D. J., Kapur, A., et al. 2023, PASA, 40, e049